



Adsorptive removal of tartrazine and methylene blue from wastewater using melamine-formaldehyde-tartaric acid resin (and a discussion about pseudo second order model)

Ahmad Baraka

Egyptian Armed Forces, Cairo, Egypt
Tel. +202 29283998; email: brkamtc@yahoo.com

Received 14 May 2011; Accepted 13 September 2011

ABSTRACT

In this study, a new resin Melamine-Formaldehyde-Tartaric acid (MF-T) was synthesized to investigate the removal of tartrazine (TZ) and methylene blue (MB) dyes. The resin was chemically, physically and morphologically characterized using IR, BET, SEM, TGA, and water content analyses. Kinetics and isotherms of TZ and MB adsorption by MF-T were studied applying batch method. Adsorption-rate data was modeled by pseudo first order (PFO) and pseudo second order (PSO) kinetic models. It was concluded that the rate of adsorption follows PSO model for both dyes. Isotherm study suggests Freundlich and Langmuir models to represent adsorption of TZ and MB respectively at equilibrium. Thermodynamic study revealed that adsorption of TZ and MB onto MF-T is spontaneous. Adsorption is exothermic for TZ in the range 15–30°C and endothermic in the range 30–45°C while it is exothermic for MB over the whole temperature studied range; 15–45°C. The regeneration experiment of MF-T by a physical treatment indicated the ease of desorbing MB from MF-T surface compared to TZ. From kinetic, isotherm, thermodynamic and regeneration studies, it is revealed that physical adsorption is the predominant removal mechanism for TZ at low temperature range and a chemical/physical adsorption process is postulated at higher temperature range. For MB, it is proposed that physical adsorption is the sole removal mechanism over all studied temperature range. It is concluded that MF-T is suitable to remove MB. The present work gives evidence that PSO model can fit both physical and chemical adsorption processes.

Keywords: Polymeric resin; Chemical; Physical; Adsorption; Pseudo-second order model; Dyes

1. Introduction

Many industrial activities (textile, leather, printing, carpet, foodstuff, etc.) produce wastewaters containing considerable amounts of coloring dyes which are often toxic and even carcinogenic. In general, they are chemically stable and poorly biodegradable due to aromaticity [1,2]. Accumulation of such materials in water bodies is recognized in many developing countries due to random discharge.

Removal of dyes before wastewater discharge is important. Adsorption is an effective remediation process to remove pollutants including dyes. In the present work, new porous polymeric resin melamine-formaldehyde-tartaric acid (MF-T) was synthesized [3,4]. Chemically, this resin is chelating and has the potential to remove some heavy metals from wastewater. Similar chelating resins (melamine-formaldehyde-NTA and

melamine–formaldehyde-DTPA) have been synthesized for the removal of M(II) from wastewater [4,5]. MF-T may also be classified as macroporous adsorbent due to its open matrix structure which gives it the capability to remove organic pollutants, [6]. Using this type of resin to remove organic compounds beside M(II) may suggest its universal water-decontamination use.

This study investigates the potential application of MF-T for removing dyes from wastewater. Two types of dyes were used, tartrazine (TZ, a yellow synthetic azo-dye) and methylene blue (MB, a blue basic bright thiazine dye). They have high potential to contaminate water because of high solubility and their wide use as coloring agents.

In addition, depending on the adsorption behavior of MF-T towards these dyes and referring to some published papers a discussion about PSO model to describe chemical and physical adsorption processes is introduced. It is important to consider this subject as it is clearly observed that this model is suggested to successfully represent the rate of adsorption for many different kinds of adsorbates (metal ions, organic compounds...) towards many different kinds of adsorbents (active carbons, inorganic minerals, biosorbents, etc.) [7]. The model assumes occurrence of chemical interaction between adsorbate and adsorbent [8], meanwhile it is unlikely necessarily that chemical interaction being the sole mechanism of adsorption for all these varieties of adsorbates and adsorbents. It is believed that PSO model is able to fit both physical and chemical adsorption processes.

2. Experimental

2.1. Theory

2.1.1. MF-T resin preparation

The matrix of melamine-formaldehyde resin (MF) is produced by acid-catalyzed methylation of melamine at elevated temperature (90–150°C) [3–5,9–12]. During bridging melamine molecules, tartaric acid react with amine groups ($-\text{NH}_2$) of melamine forming amide covalent bond. This process anchors tartaric acid to the matrix forming the rigid-porous polymeric MF-T resin [3,4,13,14].

2.1.2. Dye adsorption onto MF-T

Pseudo-first order (PFO) and pseudo-second order (PSO) models were applied to interpret the kinetic experimental data. The integral forms of PFO and PSO models have the following linear equations [8]:

$$\text{PFO: } \log(q_e - q_t) = \log q_e - \left(\frac{k_1}{2.303} \right) t \quad (1)$$

$$\text{PSO: } \frac{t}{q_t} = \frac{1}{k_2 q_e^2} + \frac{t}{q_e} \quad (2)$$

where q_e and q_t (mg g^{-1}) are the adsorbate amounts adsorbed at equilibrium and time t respectively. The parameters k_1 (1 min^{-1}) and k_2 ($\text{g mg} \cdot \text{min}^{-1}$) are models rate constants. The experimental adsorption capacity, q_{exp} (mg g^{-1}), at equilibrium was calculated using the following equation:

$$q_{\text{exp}} = (C_i - C_e) \frac{V}{M} \quad (3)$$

where C_i (mg l^{-1}) is the initial concentration, V (l) is solution volume and M (g) is the mass of the adsorbent. The estimated q_e values were compared to the calculated q_{exp} values.

Nature of adsorbent surface, its capacity and type of interaction towards certain adsorbate can be determined by studying adsorption isotherm. Linear forms of Freundlich and Langmuir adsorption isotherm models were applied in this work [15,16]:

$$\text{Freundlich: } \log q_e = \log K_F + \frac{1}{n \log C_e} \quad (4)$$

$$\text{Langmuir: } \frac{1}{q_e} = \frac{1}{Q_o} + \frac{1}{b Q_o C_e} \quad (5)$$

where q_e (mg g^{-1}) is the amount of contaminant adsorbed at equilibrium and C_e (mg l^{-1}) is the concentration of contaminant at equilibrium. The Freundlich parameters, K_F and n , are related to the adsorption capacity and intensity respectively. The Freundlich model considers multilayer adsorption and that adsorbent surface is heterogeneous. Q_o (mg g^{-1}) is the maximum adsorption capacity and b (l mg^{-1}) is related to energy of adsorption. Langmuir model assumes saturated monolayer adsorption, homogeneous adsorbent surface and inhibition of transmigration of adsorbate on that surface.

For thermodynamic study, the adsorption equilibrium stability constant was determined applying the following formula: $K_c = (C_i - C_e)/C_e$ [17,18]. The Gibbs free energy of the adsorption (ΔG_{ads}) was calculated using the Van't Hoff equation:

$$\Delta G_{\text{ads}} = -RT \cdot \ln K_c \quad (6)$$

Enthalpy (ΔH_{ads}) and entropy (ΔS_{ads}) of adsorption were calculated from the slope and intercept of the plots of $\ln K_c$ versus $1/T$ according to the following equation:

$$\ln K_c = \left(\frac{\Delta S_{\text{ads}}}{R} \right) - \left(\frac{\Delta H_{\text{ads}}}{RT} \right) \quad (7)$$

The aim of thermodynamic study is to determine the spontaneity and heat direction of adsorption process. Besides, this study can help in understanding the nature of adsorption.

2.2. Materials and procedures

2.2.1. Chemicals and adsorption measurements

Melamine 99% (Aldrich), formaldehyde 38% (BDH), tartaric acid 99% (Sigma), TZ (El-Nasr chemicals) and MB (hydrated monovalent chloride salt, Aldrich) were used in this work. Deionized water was used for MF-T synthesis, washing and regeneration and for TZ and MB solutions preparation. The following sets and instruments were used in this study: Lab. Companion SI-300R shaker to carry out adsorption experiments at specified temperature and revolutions per min., Hanna instrument pH-meter (HI8519) to measure and to adjust pH values according to experiment and Shimadzo double beam spectrophotometer (UV-120-02) for measuring TZ (at 426 nm) and MB (at 664 nm) absorbance values in their respective solutions. For each dye, a standard calibration curve was determined to compute the respective concentrations.

2.2.2. Preparation of the MF-T resin

To a vial (50 ml) containing 25 ml of strongly acidified water (pH 1.1), melamine (6.3 g) and tartaric acid (2.5 g) were added and agitated until forming dense suspension. Formaldehyde (10 ml) was added to the suspension and vial was tightly closed. The vial was again agitated until formation of homogenous white thick slurry. The vial was then placed in preheated oven at 120°C. After 5 min a slightly viscous, clear and colorless gel is produced. After 15 min, the gel solidified into white monolithic MF-T resin. The resin was left for an extra 30 min for more curing at same temperature and then left longer for about 24 h on bench at room temperature. The resin sample was ground and the formed grains were washed several times (agitation with 500 ml hot ($\approx 95^\circ\text{C}$) water for an hour) until pH became nearly neutral. Excess water was removed by centrifugation leaving grains with its intrinsic water only. Grains were then sieved and each fraction was kept in a tightly closed vial.

2.2.3. MF-T resin characterization

To determine intrinsic water content, a sample of MF-T grains (fraction: 355–710 μm) was soaked in water for 48 h to ensure water content equilibrium. Excess water was removed by centrifugation for 45 min at 1000 rpm and then weighed. Same sample was dried at 50°C for 72 h and reweighed. The difference between the two weights gives the intrinsic water content applying next equation [3]:

$$W\% = (W_w - W_d) \times \frac{100}{W_w} \quad (8)$$

where W_w and W_d are the wet and dry weights of the resin respectively.

Freeze-dried sample of MF-T was used for BET analysis and SEM imaging. The Micromeritics ASAP 2405 N adsorption analyzer was used for measuring nitrogen adsorption/desorption isotherms at 77.4 K to determine the porosity of the sample. SEM imaging of the outer surface of MF-T grains was performed using FE-SEM (Model S-900, Hitachi, Ltd) to investigate surface morphology and porosity (magnification of $\times 2500$ and accelerating voltage of 25 kV).

IR measurements were performed in the range 400–4000 cm^{-1} (applying KBr-disc technique using a Perkin-Elmer FT-IR spectrometer) for three conventionally dried samples: MF-T, MF-T-C (resin bearing TZ due to adsorption at 15°C) and MF-T-W (resin bearing TZ due to adsorption at 45°C). This analysis was performed to investigate the adsorption nature of TZ onto MF-T.

Thermo-gravimetric analysis was performed using semi-dried samples of MF-T, MF-T-C and MF-T-W (using Shimadzu TGA-50H: under a continuous argon flow of 100 ml min^{-1} , heating from room temperature to 500°C with 10°C min^{-1} heating rate). Thermo-graphs were studied to help suggest if TZ adsorption onto MF-T is chemical or physical.

2.2.4. TZ and MB adsorption

Stock solutions of TZ (100 ppm) and MB (50 ppm) were prepared by dissolving respective amounts of each dye in 1000 ml water. Other working solutions were prepared by appropriate dilutions. Batch method was conducted for all adsorption experiments with some conditions were kept fixed: dye solution volume (50 ml in 250 ml conical flask), sample agitation rate (100 rpm) and pH of dye solution (6.7 ± 0.02). MF-T has been used in hydrated form with grain size (355–710 μm). For kinetic studies, 0.2 g of MF-T was used for each experiment. For TZ-isotherm study 0.1 g of MF-T was used for each experiment and for MB-isotherm study 0.025 g of MF-T was used for each experiment.

Kinetic studies were performed at three different temperatures: 15, 30 and 45°C and each sample had initial concentration of 50 and 10 ppm for TZ and MB respectively. Every 10 min (for a total period of 90 min) a liquor sample of 1.5 ml was withdrawn from sample flask with a micropipette. The absorbance was measured and the liquor volume was directly returned back to the sample flask. Adsorption isotherm studies were performed at 30°C using five initial concentrations for TZ: 30, 40, 50, 60, and 70 ppm and five initial concentrations for MB: 10, 20, 30, 40 and 50 ppm. Liquor samples were

withdrawn at equilibrium and absorbance values were recorded. For the thermodynamic study, the adsorption equilibriums (TZ initial concentration: 50 ppm and MB initial concentration: 10 ppm) were investigated for temperatures of 15°C, 22.5°C, 30°C, 37.5°C and 45°C.

2.2.5. Regeneration of MF-T

Preloaded samples of MF-T at 25°C by TZ ($C_i = 50$) and MB ($C_i = 10$) were treated five times each by hot water (50 ml at 90°C) for an hour to investigate the adsorption nature of each dye. The absorbance of treating water for each cycle was determined to find out extent of dye release. Besides, MF-T treated samples were photographed after treatment to visualize apparent remains of these two dyes.

3. Results and discussion

3.1. General

MF-T grains are rigid and white. Upon adsorption of TZ and MB, separately, its color changed into yellow and blue respectively. This may suggest that adsorption is solely physical for both dyes.

3.2. Characterization of MF-T resin

Intrinsic water content of MF-T was found to be about 53.89 mmol g^{-1} ($W\% \approx 96.8$). This high value suggests that MF-T surface is strongly hydrophilic [19]. The hydrophilic character is due to presence of non-reacted carboxylic, amide and non-reacted amine groups present in matrix structure. This character facilitates migration of solution inside pores and causes rapid adsorption of pollutants [20].

BET analysis gave the porosity characteristics of MF-T as given in Table 1. Surface area is limited (23.4 $m^2 g^{-1}$) and consequently cumulative pore volume is limited. However, the average pore diameter (12.5 nm) is large enough for dye migration in pores (TZ length: 20.6 Å [21] and MB area: 132 Å² [22]). It is suggested that dominant pores are meso- and macro- porous as micropore surface area is extremely small. Macroporous resins are highly

Table 1
Porosity characteristics of MF-T

Character	Value
Total BET surface area ($m^2 g^{-1}$)	23.4
BET Micropores (<2 nm)	0.1
BJH Adsorption cumulative pore volume ($cm^3 g^{-1}$)	0.072
Total average pore diameter (nm)	12.5

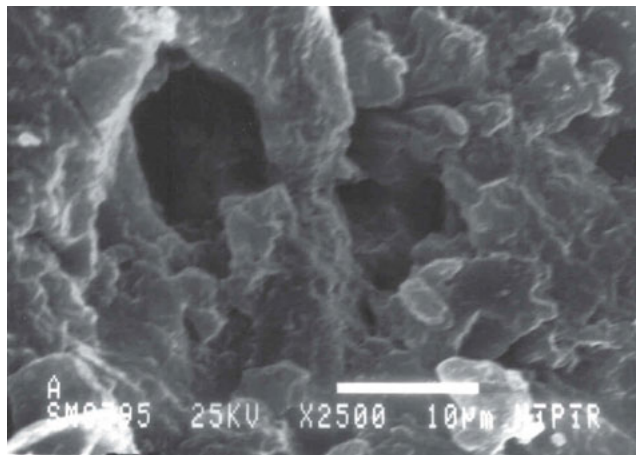


Fig. 1. SEM image of MF-T grain outer surface.

dedicated for the removal of large organic molecules from wastewater [23,24]. Fig. 1 shows the SEM image of the outer surface of MF-T sample. Irregular and large pores are clearly seen. This porosity is responsible for considerably high rate of dye adsorption.

Summary of TGA analysis is given in Table 2. The MF-T-C sample has significant differences in midpoints, onsets, endsets and weight losses compared to MF-T and MF-T-W. Markedly, weight loss scenario for MF-T-C is different. This may be due to presence of two distinct masses which indicates physical adsorption of TZ onto MF-T. On the other hand, R1 and R3 columns of MF-T and MF-T-W are almost similar. TZ in this case is suggested to be chemically anchored to MF-T in MF-T-W sample and one mass is present which resembles

Table 2
Data of TGA measurements for MF-T, MF-T-C and MF-T-W

Character	MF-T			MF-T-C			MF-T-W		
	R1	R2	R3	R1	R2	R3	R1	R2	R3
Mid point (°C)	70.97	269.2	329	85.11	357.1	475.9	66.36	–	329.7
Onset (°C)	47.68	256.1	323.9	65.7	349.4	473.7	46.7	–	321.9
Endset (°C)	97.42	288.4	335.8	115.7	366.9	525.7	89.17	–	341.6
Weight loss%	–18.5	–8.5	–21.5	–52.9	–15.6	–4.15	–13.6	–	–15.6

MF-T. MF-T-C sample shows the highest weight loss (52%) at 85.11°C which may be due to evaporation of TZ-hydrating water. This amount of water can be present only when TZ is physically adsorbed. TGA may indicate that TZ has a chemical interaction with MF-T at high temperature while at low temperature the adsorption is physical.

Also, an important note can be driven considering both kinetic and TGA studies. Kinetic gave that the difference in TZ removal percentage for the two cases MF-T-C and MF-T-W is only about 5%. And, TGA showed different graphs for MF-T-C and MF-T-W. If TZ is present in both samples by the same mechanism, both samples should give very similar graphs because of similar removal percentage.

3.3. Adsorption kinetics

TZ and MB removal rates are shown in Figs. 2 and 3 respectively. After 10 min., TZ removal percentage exceeded 60% and MB removal percentage was about 40–50% for different temperatures. These high removal

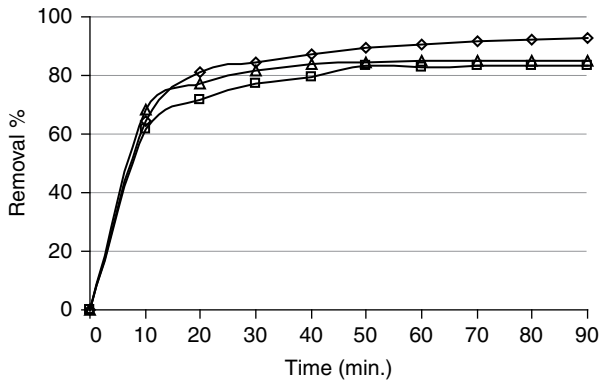


Fig. 2. TZ removal rate by MF-T at $T = 15$ (\diamond), 30 (\square) and 45°C (Δ) and initial concentration 50 ppm.

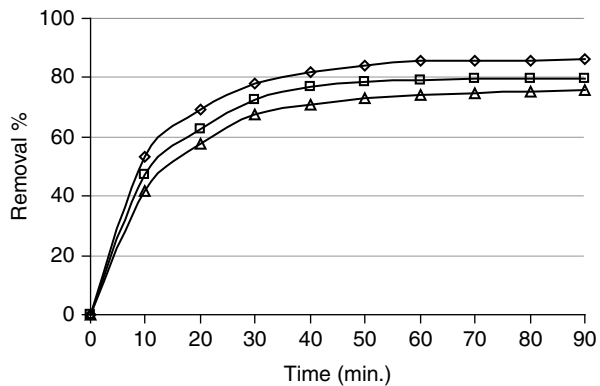


Fig. 3. MB removal rate by MF-T at $T = 15$ (\diamond), 30 (\square) and 45°C (Δ) and initial concentration 10 ppm.

percentages are due to open structure and high hydrophilicity of MF-T. For MB as temperature decreased, the rate of adsorption increased which indicate exothermic process and this is compatible with physical adsorption. For TZ, adsorption rates at 15°C and 45°C are higher than the rate at 30°C . This indicates that TZ adsorption mechanism changes with temperature. It can be observed that MB-removal increases regularly with time which is not the case for TZ. This observation may suggest stable single mechanism for MB-adsorption and complex mechanism for TZ-adsorption.

Kinetic plots of PFO and PSO are given in Figs. 4–7 applying linear regression method using regression tool of Microsoft Excel program. From plots the parameters of each model, correlation factors (r) and standard errors (SE) were determined and they are summarized in Table 3. All correlation factors are significant as the probability that variables are uncorrelated was found to be less than 5% and linearity with 95%-confidence was concluded [25]. Comparing values of correlation factor solely is not adequate to select a model that gives best fit of data [7]. To assess the quality of model fitness with

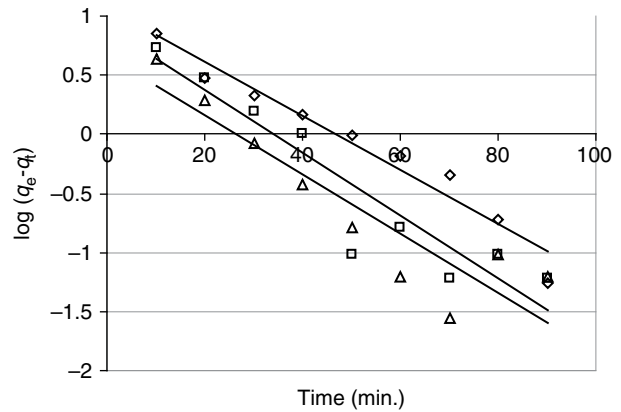


Fig. 4. PFO plots for TZ adsorption onto MF-T at $T = 15$ (\diamond), 30 (\square) and 45°C (Δ) and initial concentration 50 ppm.

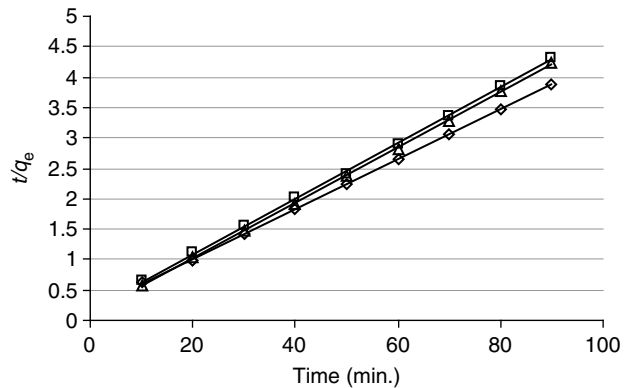


Fig. 5. PSO plots for TZ adsorption onto MF-T at $T = 15$ (\diamond), 30 (\square) and 45°C (Δ) and initial concentration 50 ppm.

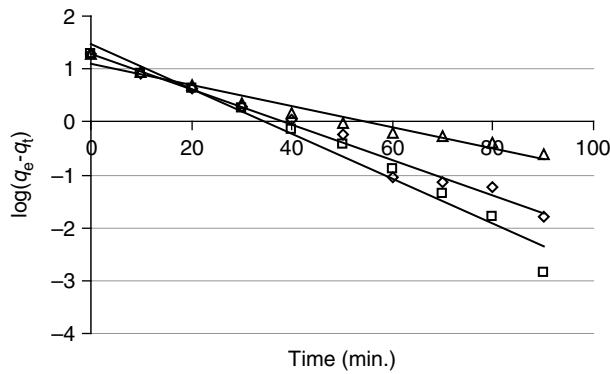


Fig. 6. PFO plots for MB adsorption onto MF-T at $T = 15$ (\diamond), 30 (\square) and 45°C (Δ) and initial concentration 10 ppm.

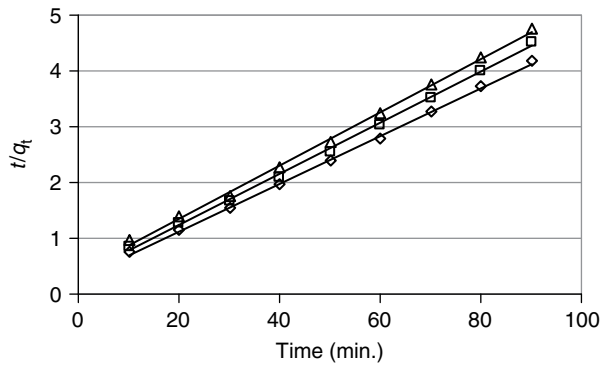


Fig. 7. PSO plots for MB adsorption onto MF-T at $T = 15$ (\diamond), 30 (\square) and 45°C (Δ) and initial concentration 10 ppm.

experimental data, capacity at equilibrium (q_e), correlation factors, and SE were considered.

From Table 3; q_e values with respect to corresponding q_{exp} values, r values and SE values assign PSO to represent the kinetics of TZ and MB removal. According to Ho and McKay [8], a sort of chemical interaction involving electrons sharing and/or exchange between these dyes and functional groups of MF-T can be expected [26–28]. Besides, boundary layer resistance is considered to have limited effect because of MF-T open structure. Although PSO suggests a chemical adsorption, revising its parameters may indicate something different. For TZ, initial sorption rate ($h = k_2 q_e^2$) and overall rate (k_2) have the highest values at 45°C . This indicates chemical-step dependent process especially at this temperature. However, the increase in temperature did not cause an increase in q_e value which suggests specified area and limited functionality of MF-T to chemically bond TZ. That is, for TZ, the chemical interaction can be considered. TZ have functional groups that can chemically react with MF-T. In fact, the decrease in q_e can be related to desorption of some physically adsorbed TZ. For MB, h continuously decreases and k_2 slightly decreases with temperature which indicates physical adsorption. Besides, increase in temperature caused a decrease in q_e value which also suggests no chemical reaction. Instead, desorption rate is believed to increase as temperature increases, and that is why q_e decreases. That is, for MB, physical adsorption is the main mechanism of removal and chemical interaction is limited or not

Table 3
Kinetics data fitting of TZ- and MB-removal according to PFO and PSO models

Temp. ($^\circ\text{C}$)	C_i (ppm)	q_{exp} (mg g^{-1})	Pseudo first order				Pseudo second order			
			k_1 (min^{-1})	q_e (mg g^{-1})	r	SE	k_2 ($\text{g mg} \cdot \text{min}^{-1}$) h (mg/g min)	q_e (mg g^{-1})	r	SE
For TZ										
15	50	23.3	0.0527	11.69	0.9547	0.1614	8.7×10^{-3} 5.216	24.45	0.9999	0.0129
30		20.9	0.0610	7.88	0.8750	0.2999	1.2×10^{-2} 5.565	21.93	0.9995	0.0298
45		21.3	0.0576	4.53	0.8402	0.3554	2.0×10^{-2} 9.443	21.95	0.9998	0.0211
For MB										
15	10	21.40	0.0778	19.93	0.9815	0.14931	6.7×10^{-3} 3.647	23.36	0.9990	0.04006
30		19.96	0.0976	29.70	0.9715	0.23324	6.7×10^{-3} 3.179	21.79	0.9981	0.05843
45		18.96	0.0461	12.47	0.9660	0.12063	5.7×10^{-3} 2.493	20.92	0.9984	0.05578

present at all. MB does not have suitable chemical groups to interact with MF-T.

The conclusion here is that although PSO apparently suggests that both dyes were subjected to some sort of chemical-interaction with MF-T, the detailed discussion about its parameters suggests different adsorption behavior of both dyes.

3.4. Adsorption isotherms

The Figs. 8 and 9 show the removal at equilibrium (q_e) of TZ and MB against equilibrium concentration (C_e) of these dyes at 30°C respectively. For both dyes, regular concave increase of plots is observed which indicates initial rapid increase in adsorption process [29,30]. This is in agreement with outputs of kinetic study.

Figs. 10–13 present the linear plots of adsorption isotherm according to the Freundlich and Langmuir models. From these plots the parameters of each model, r values and SE values were determined by linear regression and are presented in Table 4. For both dyes, the two models show significant correlation with experimental data and linearity with 95%-confidence was concluded [25].

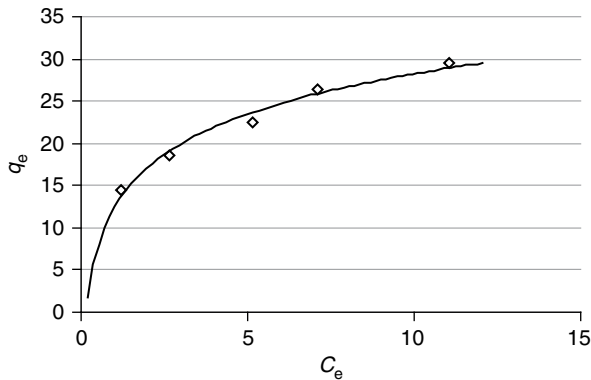


Fig. 8. Adsorption isotherm (at 30°C) of TZ onto MF-T with initial concentrations: 30, 40, 50, 60 and 70 ppm.

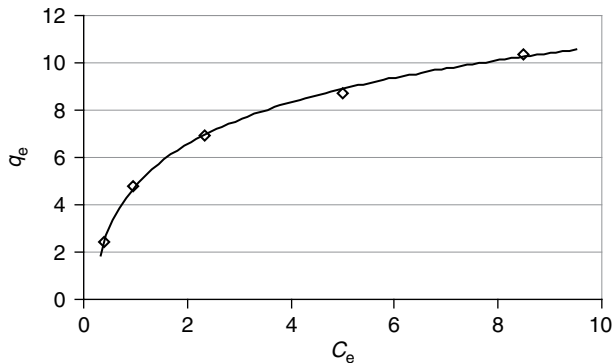


Fig. 9. Adsorption isotherm (at 30°C) of MB adsorption onto MF-T with initial concentrations: 10, 20, 30, 40 and 50 ppm.

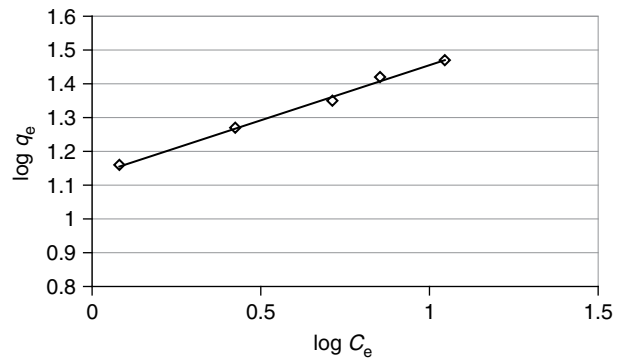


Fig. 10. Freundlich adsorption isotherm of TZ onto MF-T (at 30°C).

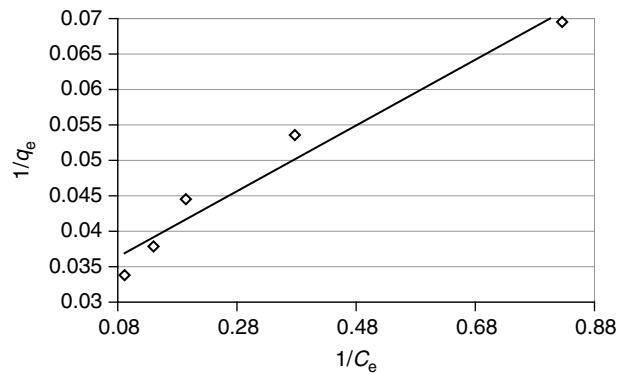


Fig. 11. Langmuir adsorption isotherm of TZ onto MF-T (at 30°C).

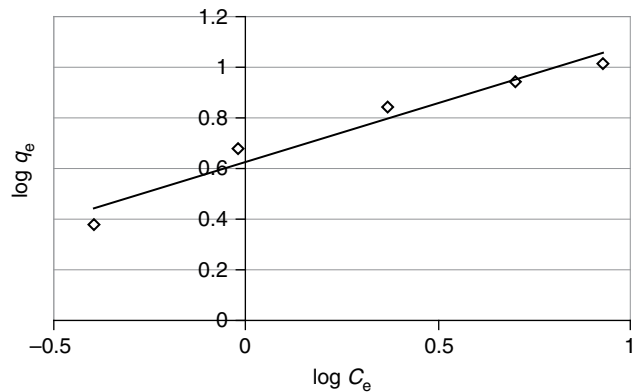


Fig. 12. Freundlich adsorption isotherm of MB onto MF-T (at 30°C).

Regarding Freundlich model, n value for TZ adsorption is higher than that of MB. This may indicate that chemical adsorption is more probable for TZ than for MB [31]. Regarding Langmuir model, TZ adsorption onto MF-T shows maximum capacity of 21.6 mg g⁻¹. For MB, maximum capacity is 60.6 mg g⁻¹ which is obviously higher than that of TZ.

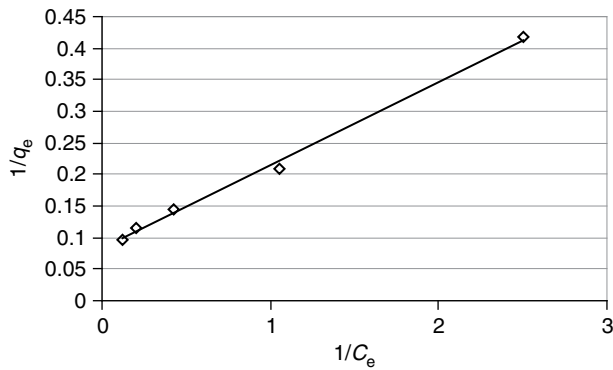


Fig. 13. Langmuir adsorption isotherm of MB onto MF-T (at 30°C).

Table 4
Data-fitting of TZ-adsorption isotherm (30°C) by Freundlich and Langmuir models

Dye	Freundlich	Langmuir
TZ	$k_F ((\text{mg g}^{-1})(\text{mg l}^{-1})^n) = 13.5$ $1/n = 0.3277$ ($n \approx 3.05$) $r = 0.9971$ $SE = 0.0109$	$Q_o (\text{mg g}^{-1}) = 21.6$ $b (\text{l mg}^{-1}) = 0.7084$ $r = 0.9789$ $SE = 0.0067$
MB	$k_F ((\text{mg g}^{-1})(\text{mg l}^{-1})^n) = 33.8$ $1/n = 0.4608$ ($n \approx 1.41$) $r = 0.9778$ $SE = 0.06124$	$Q_o (\text{mg g}^{-1}) = 60.6$ $b (\text{l mg}^{-1}) = 0.6303$ $r = 0.9984$ $SE = 0.00835$

To assess the quality of the fitness of a model, r and SE values were considered. For TZ, Freundlich model shows higher correlation factor and higher SE compared to those of Langmuir model. Here, r value suggest Freundlich model to represent the adsorption process, while SE value is against this suggestion. This leads to conclude that single mechanism of adsorption can not be suggested and some sort of energy non-homogeneity is predicted for MF-T surface towards TZ. This idea can be supported by denoting that PSO suggested the same. For MB, Langmuir model has lower SE and higher correlation factor than those given by Freundlich model. Here, both r and SE suggest Langmuir to represent the adsorption process. Accordingly, monolayer physical adsorption is highly predicted and MF-T is considered to have homogenous surface with respect to MB. Hence, the suggestion by PSO model that MB should chemically react with MF-T surface (kinetic discussion) is not applicable.

As a conclusion, MB adsorption is suggested to be monolayer physical process following Langmuir model

and TZ adsorption is suggested to be monolayer chemical process following Freundlich model.

3.5. Thermodynamic studies

Fig. 14 shows the plots of $\ln K_c$ against $1/T$ for TZ adsorption. As shown, the adsorption changes with temperature and two ranges can be identified: 15–30°C and 30–45°C. Exact mid-point between the two ranges may not be specified at 30°C, but it is likely to be close [3].

Table 5 summarizes enthalpy and entropy changes of TZ adsorption. For 15–30°C range, ΔH_{ads} is negative meaning exothermic adsorption process. Its comparatively small value (5.73 kJ mol⁻¹) can indicate dominating of physical-adsorption mechanism in this range with minor contribution of chemical-adsorption mechanism. It is also clear from Fig. 2 that adsorption at 15°C is the highest which suggests strong physical adsorption at low temperature. For 30–45°C range, ΔH_{ads} is positive with a comparatively very low value (1.17 kJ mol⁻¹). Positivity may indicate a complicated physical/chemical adsorption mechanism with overall endothermic behavior. In this particular condition, it can be hypothesized an endothermic chemical interaction which consumes energy emerged from the accompanying exothermic physical interaction. That is, chemical part slightly overweighs the contribution of exothermic physical part.

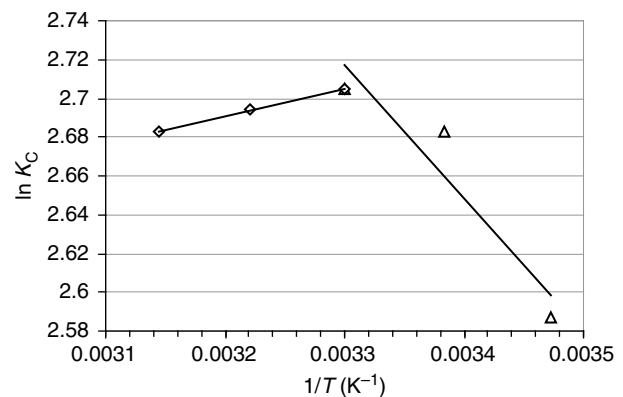


Fig. 14. Plots of $\ln K_c$ against $1/T$ for TZ adsorption onto MF-T.

Table 5
TZ adsorption thermodynamic parameters, ΔH_{ads} and ΔS_{ads}

Temp. Range	15–30°C	30–45°C
ΔH_{ads} (kJ mol ⁻¹)	-5.73	+1.17
ΔS_{ads} (J mol ⁻¹ K ⁻¹)	+41.51	+18.63
r	0.8930	0.9969

TZ molecule includes two sulphonate groups ($-\text{SO}_3\text{Na}$) and one carboxylate group ($-\text{COONa}$) that would react covalently with MF-T groups such as carboxylic group ($-\text{COOH}$), hydroxyl groups ($-\text{OH}$) and linking amine ($-\text{NH}$) [32]. There are some probable chemical reactions that may occur between TZ and MF-T. However, sulphonate reaction with amine producing sulphonamide is the most probable due to gentle heating ($30\text{--}45^\circ\text{C}$) [33]. This postulated reaction was supported by simple auxiliary experiment in which pH value of a liquor sample was determined before and

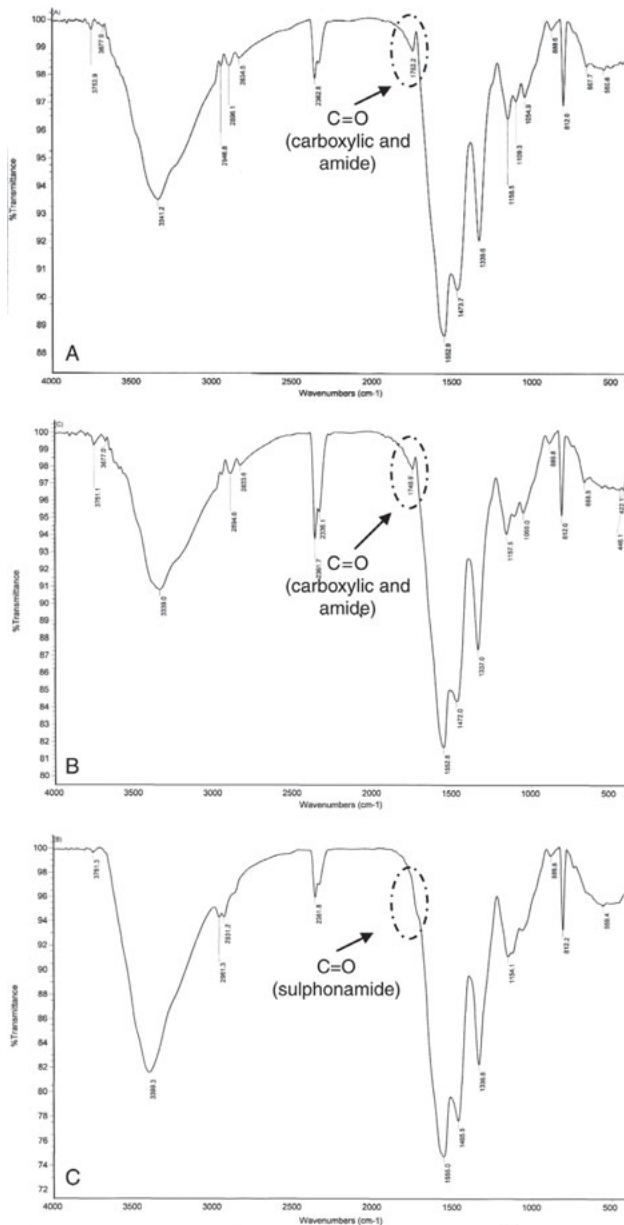


Fig. 15. IR spectra of (a) MF-T, (b) MF-T-C and (c) MF-T-W resins.

after TZ-adsorption at 45°C . A measurable increase of about $0.1 (\pm 0.02)$ was detected (this experiment was performed three times) and can be explained by the release of NaOH. The increase in pH value is small due to the small used amount of MF-T in the experiment.

IR analysis may help in understanding TZ chemical adsorption behavior at 45°C by considering IR spectra of MF-T, MF-T-C and MF-T-W as shown in Fig. 15. The spectra of MF-T, MF-T-C are almost identical which means domination of physical adsorption (TZ does not clearly attribute in the second spectrum due to its very low mass percentage in the sample). On the contrary, the comparison of IR spectra of MF-T and MF-T-W gives marked difference at 1752.2 cm^{-1} (carbonyls of carboxylic group and amide group of matrix-pendent TZ). This peak is slightly masked by 1552.9 cm^{-1} band, spectrum (C), however, has a recognizable shoulder due to shift of $\text{C}=\text{O}$ to lower value. Hence, sulphonate reaction with amine producing sulphonamide is highly predicted to occur [34]. Although TZ is also of low mass percentage in this sample, it spread and reacted with most of surface-amine groups.

The azo group which is responsible for the color of TZ did not take part in the reaction and that is why the color did not change with this chemical adsorption as given in Section 3.1.

For $15\text{--}30^\circ\text{C}$ range, ΔS_{ads} is positive and indicates increase in disorder during adsorption of TZ from solution to MF-T surface. Adsorption of TZ molecule itself on MF-T causes more order. But in addition, during adsorption the hydrating water spheres (TZ is highly hydrated due to presence of negatively two sulphonate groups and a carboxylate group) is librated and becomes mobile in aqueous phase which increases disorder [4]. For $30\text{--}45^\circ\text{C}$ range, ΔS_{ads} is also positive following same mechanism and it is plausible to conclude that the adsorption of TZ is entropically driven for both cases [35]. However, its value is less in latter case due to less water-molecules librated as TZ is already less hydrated for this hot range.

ΔG_{ads} values are negative confirming spontaneous nature of adsorption process in the studied temperature span (Table 6). Absolute value increases with temperature which indicates more contribution of chemical adsorption mechanism [36].

Fig. 16 shows the plots of $\ln K_c$ against $1/T$ for MB adsorption onto MF-T. From the figure, it can be concluded

Table 6
TZ adsorption free energy, ΔG_{ads}

Temp. ($^\circ\text{C}$)	15	22.5	30	37.5	45
ΔG_{ads} (kJ mol^{-1})	-6.18	-6.58	-6.80	-6.94	-7.08

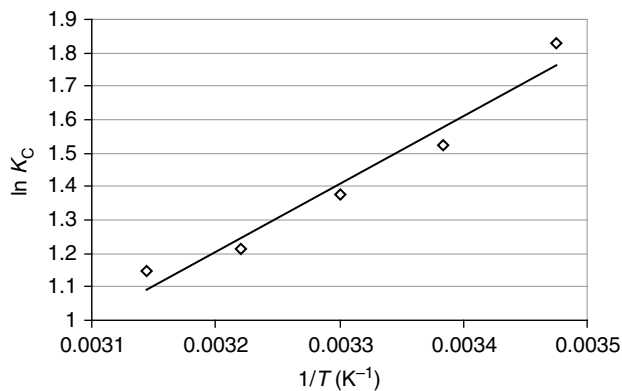


Fig. 16. Plots of $\ln K_c$ against $1/T$ for MB adsorption onto MF-T.

Table 7

MB adsorption thermodynamic parameters, ΔH_{ads} and ΔS_{ads}

Temp. range	15–45°C
ΔH_{ads} (kJ mol ⁻¹)	-16.96
ΔS_{ads} (J mol ⁻¹ K ⁻¹)	-44.27
r	0.9582

that adsorption performance is stable with temperature and increases as temperature decreases. This suggests a physical adsorption supporting outputs of kinetic and isotherm studies [36].

Table 7 summarizes the enthalpy and entropy changes upon MB adsorption. ΔH_{ads} is negative indicating exothermic adsorption and its value (16.96 kJ mol⁻¹) can indicate strong physical process as a mechanism. Besides, it is considered strong as there is some energy consumed for dehydration. Upon adsorption, the MF-T became blue suggesting no chemical reaction with the aromatic sulfur containing part. ΔS_{ads} is negative indicating increase in order during adsorption of MB. This may be due to less hydration of MB compared to TZ. Also, this suggests that MB adsorption is enthalpy driven [37]. Although the negative entropy change indicates resistance to adsorption process, it also indicates ease of regeneration [4].

According to Table 8, ΔG_{ads} values are negative confirming spontaneity of adsorption. However, the absolute

Table 8

MB adsorption free energy, ΔG_{ads}

Temp. (°C)	15	22.5	30	37.5	45
ΔG_{ads} (kJ mol ⁻¹)	-4.36	-3.74	-3.46	-3.13	-3.03

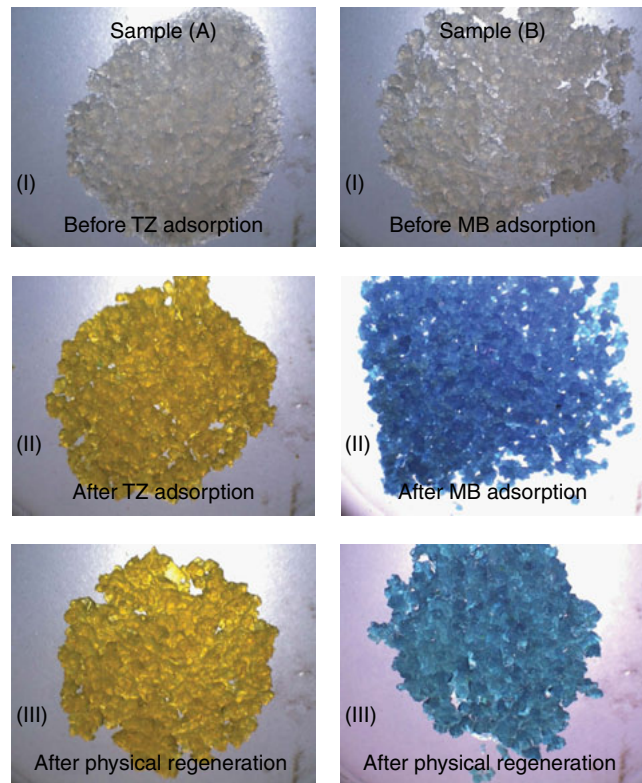


Fig. 17. Samples (a) and (b) of MF-T resin, (I) before adsorbing, (II) after adsorbing and (III) after physical regeneration.

value increases as temperature decreases which indicates favoring lower temperatures. This strongly suggests physical adsorption.

3.6. Regeneration of MF-T (removing TZ and MB)

Fig. 17 (I) shows two samples of MF-T. Both are identical as they did not adsorb dyes yet. Fig. 17 (II) shows the apparent color intensity of the same resin samples after equilibrium-adsorption of TZ by sample (A) and of MB by sample (B). After hot-water treatment, the color of TZ-adsorbing sample almost retains its intensity whereas MB-adsorbing sample shows that color diminished to distinguishable extent as shown in Fig. 17 (III).

To quantify these observations, the absorbance values of treating waters were measured to find out if dyes were released. Table 9 gives these absorbance values. According to these values, it can be claimed that TZ did not notably desorb by hot water and on the contrary, MB shows considerable desorption by this physical treatment method. Although the calculated total desorption of MB is about 57%, the fact that physical desorption succeeded to remove some detectable amount of

Table 9
Absorbance (water of treatment) of TZ and MB (Adsorption at 25°C)

	Abs. (TZ)	Abs. (MB)
Initial conc.	0.727 (50 ppm)	1.705 (10 ppm)
Equilibrium conc. (24 h)	0.123	0.351
Corresponding adsorbed at equilibrium	$0.727 - 0.123 = 0.604$	$1.705 - 0.351 = 1.354$
Desorption cycle # (1 h at 90°C)	Abs. (TZ)	Abs. (MB)
Cycle 1	No read	0.398
Cycle 2	No read	0.201
Cycle 3	No read	0.113
Cycle 4	No read	0.05
Cycle 5	No read	0.01

MB from MF-T is still verified. The limited percentage of desorption may be due to the strong physical adsorption ($\Delta H_{\text{ads}} = -16.96 \text{ kJ mol}^{-1}$) which causes some resistance to remove MB from resin surface.

The subject of color observations and absorbance measurements support the idea that TZ was chemically (partially or totally) adsorbed and MB was physically adsorbed. It is recommended to use MF-T for the removal of dyes that physically adsorb because of the potential simple regeneration technique.

From regeneration, isotherm and thermodynamic studies; MF-T chemically adsorbed TZ and physically adsorbed MB. On the contrary, kinetic study suggested that MF-T chemically adsorb both. This can be considered as confliction; hence a discussion about PSO model to successfully express physical mechanism as well as chemical mechanism is given in the next section.

3.7. PSO model and chemical/physical postulation

In some published papers in which PSO was suggested to well represent the kinetic data [38–41], authors directly concluded that adsorption occurs due to “chemical sorption or chemisorption involving valency forces” as Hoand McKay. presented [8], without specific identification of such chemical interaction. Some other papers suggested PSO to well fit the kinetic data without giving the impact of this fitness [42–47].

According to present work, PSO is believed to represent both chemical and physical adsorption in equal terms. Under the light of kinetics, isotherms,

thermodynamics and regenerations studies, a confliction is clearly observed: kinetics of both dyes suggest PSO well fits the experimental data and consequently these two dyes, according to Hoand McKay [8] may follow a chemisorption process. Whereas isotherms, thermodynamics and regenerations experiments clearly indicate that chemical and physical adsorptions are dedicated for TZ and only physical adsorption is dedicated for MB. This means that PSO can represent chemical and physical adsorptions.

Discussing theoretical models of sorption kinetics (PSO, PFO and Elovich equations), Plazinski et al. stated that “surface reaction” term may not necessarily mean the actual chemical reaction occurring on the adsorbent surface involving the formation of chemical bonds. Interactions of physical nature (van der Waals’ forces, for instance) may also play a role [7]. In other words, they suggest that physical and chemical processes can be represented by PFO and PSO models.

Also, Azizian demonstrated mathematically that observed adsorption rate constants of PFO and PSO are not intrinsic. Instead, both are dependent on adsorption and desorption rate constants and are functions of adsorbate initial concentration [48]. This indicates reversibility character of the adsorption process which is valid for both chemical and physical processes.

Furthermore, a survey over some randomly selected works was performed. These works cover different types of adsorbent and adsorbate and all selected PSO to represent adsorption kinetics [49–60]. Table 10 gives these works. For each work, suggestions based on PSO model and adsorption enthalpy change are given. Out of these, five works does not give a clear suggestion about the nature of adsorption either based on PSO or enthalpy [49–53]. Authors may try to avoid non-consistency. Three works give suggestion based on thermodynamics and nothing about PSO [54–56] and three based on PSO and nothing about thermodynamics [57–59]. This may be to avoid confliction. Only one work gives suggestions based on both and yet they are different [60].

In general, the concept of adsorption can be regarded as *attachment* of adsorbate onto adsorbent surface regardless of the working mechanism (i.e., physical or chemical). The present work is evidence that PSO model can represent physical and chemical adsorption processes on equal terms. As a conclusion, it can be suggested that PSO model may represent “chemical adsorption involving valency forces through sharing or exchange of electrons between adsorbate and adsorbent, or physical adsorption involving intensive working van der waals’ forces between adsorbate and adsorbent surface” [7].

Table 10
Reviewed works for different adsorption systems

Reference	Absorbent	Adsorbate	PSO model best fit (R^2) and suggestion of interaction	Absolute enthalpy and authors' suggested nature of adsorption
[49]	Calix[4]arene based resin	azo dyes	$R^2 = 0.99$ and 0.99 . <i>No suggestion.</i>	$\Delta H = 36.94, 28.74 \text{ kJ mol}^{-1}$. <i>No suggestion.</i>
[50]	Princess tree leaf	Basic Red 46	$R^2 = 0.9993$. <i>No suggestion.</i>	$\Delta H = 43.76 \text{ kJ mol}^{-1}$. <i>No suggestion.</i>
[51]	Lignocellulosic waste biomass activated carbon	Amido Black 10B (AB10B)	Many R^2 all are the highest <i>No suggestion.</i>	$\Delta H = 48.194, 44.989$ and $52.129 \text{ kJ mol}^{-1}$. <i>No suggestion.</i>
[52]	Polyacrylamide	methyl violet	Many R^2 all are the highest <i>No suggestion.</i>	$\Delta H = 37.3 \text{ kJ mol}^{-1}$ <i>No suggestion.</i>
[53]	Rice husk	Direct Red-31 and Direct Orange-26 dyes	Many R^2 all are the highest. <i>No suggestion.</i>	$\Delta H = 40.846$ and $64.989 \text{ kJ mol}^{-1}$. <i>No suggestion.</i>
[54]	Activated carbon by phosphoric acid	Ni (II)	$R^2 = 0.99995, 0.99982$ and 0.99963 . <i>No clear suggestion.</i>	$\Delta H = 4.67 \text{ kJ mol}^{-1}$. <i>Physical in nature.</i>
[55]	Pine cone	Acid Black 26 (AB26), Acid Green 25 (AG25) and Acid Blue 7 (AB7)	$R^2 = 1$ for all conditions. <i>No clear suggestion.</i>	$\Delta H = 11.81, 11.04$ and 2.02 for studied dyes. <i>Physisorption according to free energy.</i>
[56]	Modified wheat residue	Reactive Red-24, RR-24	Many R^2 all are the highest. <i>No suggestion.</i>	$\Delta H = 1.704 \text{ kJ mol}^{-1}$ <i>Physical in nature</i>
[57]	Moringa oleifera bark	Ni(II)	$R^2 = 0.9971, 0.9964$ and 0.9996 . <i>Chemical in nature.</i>	$\Delta H = 12.15 \text{ kJ mol}^{-1}$. <i>No clear suggestion.</i>
[58]	Natural bentonite	Zn (II)	Many R^2 all are the highest. <i>Chemisorptions.</i>	All $\Delta H = 12.3143 \text{ kJ mol}^{-1}$. (strange data) <i>No suggestion.</i>
[59]	Nano zerovalent iron particles	Cd (II)	$R^2 = 1$ for all conditions (strange data). <i>Chemisorption.</i>	$\Delta H = 7.17 \text{ kJ mol}^{-1}$. <i>No suggestion.</i>
[60]	Activated carbon derived from loosestrife	2,4,6-trichlorophenol	$R^2 = 0.9999$ to 1 . <i>Chemisorption.</i>	$\Delta H = 12.89 \text{ kJ mol}^{-1}$ <i>Physisorption.</i>

4. Conclusions

New melamine–formaldehyde–tartaric acid adsorbent (MF-T) was synthesized and characterized to be rigid, hydrophilic and macroporous. Its surface area is limited ($\approx 23.4 \text{ m}^2 \text{ g}^{-1}$), however showed suitable capacity for the removal of TZ and MB dyes. Removal rate of TZ and MB by MF-T exceeded about 60% and 45% respectively within the first 10 min for the different studied temperatures which suggest an open matrix structure. The Freundlich model is better describing the adsorption process of TZ suggesting a chemical adsorption and Langmuir is better describing the adsorption of MB suggesting a physical adsorption. For both dyes, adsorption process is spontaneous in the studied temperature range. TZ adsorption was entropy-driven and MB was enthalpy-driven. MF-T is suitable to remove MB and similar non-reactive dyes because of simple regeneration. Although both dyes obeyed PSO model for their removal rates, it is suggested that TZ shows a chemical/physical adsorption behavior and MB shows a physical adsorption behavior. It is concluded that removal of MB and similar dyes is dedicated to be accomplished by MF-T due to simple physical regeneration method. It is suggested that PSO model can express physical adsorption as well as chemical adsorption. Investigating the changes in PSO model parameters with temperature would help understanding the adsorption nature of certain adsorbate onto certain adsorbent.

References

- [1] S. Chen, J. Zhang, C. Zhang, Q. Yue, Y. Li and C. Li, Equilibrium and kinetic studies of methyl orange and methyl violet adsorption on activated carbon derived from Phragmites australis, *Desalination*, 252 (2010) 149–156.
- [2] A. Cestari, E. Vieira, G. Vieira, L. da Costa, A. Tavares, W. Loh and C. Airoidi, The removal of reactive dyes from aqueous solutions using chemically modified mesoporous silica in the presence of anionic surfactant—the temperature dependence and a thermodynamic multivariate analysis, *J. Hazard. Mater.*, 161 (2009) 307–316.
- [3] A. Baraka, P. Hall and M. Heslop, Melamine–formaldehyde–NTA chelating gel resin: synthesis, characterization and application for copper(II) ion removal from synthetic wastewater, *J. Hazard. Mater.*, 140 (2007) 86–94.
- [4] A. Baraka, P. Hall and M. Heslop, Preparation and characterization of melamine–formaldehyde–DTPA chelating resin and its use as an adsorbent for heavy metals removal from wastewater, *React. Funct. Polym.*, 67 (2007) 585–600.
- [5] A. Baraka, Removal of heavy metals from aqueous solutions by novel melamine–formaldehyde–polyaminocarboxylic acid chelating adsorbents, PhD, The University of Strathclyde, Glasgow, 2007.
- [6] M.P. Tsyurupa, L.A. Maslova, A.I. Andreeva, T.A. Mrachkovskaya and V.A. Davankov, Sorption of organic compounds from aqueous media by hypercrosslinked polystyrene sorbents ‘Styosorb’, *React. Polym.*, 25 (1995) 69–78.
- [7] W. Plazinski, W. Rudzinski and A. Plazinska, Theoretical models of sorption kinetics including a surface reaction mechanism: a review, *Adv. Colloid Interface Sci.*, 152 (2009) 2–13.
- [8] Y.S. Ho and G. McKay, Pseudo-second-order model for sorption processes, *Proc. Biochem.*, 34 (1999) 451–465.
- [9] E. Minopoulou, E. Dessipri, G. Chryssikos, V. Gionis, A. Paipetis and C. Panayiotou, Use of NIR for structural characterization of urea formaldehyde resins, *Int. J. Adhes. Adhes.*, 23 (2003) 473.
- [10] X. Sun and Z. Chai, Urea-formaldehyde resin monolith as a new packing material for affinity chromatography, *J. Chromatogr. A*, 943 (2002) 209.
- [11] R. Baltieri, L. Innocentini-Mei, W. Tamashiro, L. Peres and E. Bittencourt, Synthesis of porous microspheres from aminopolymers, *Eur. Polym. J.*, 38 (2002) 57.
- [12] K. Mequanint and R. Sanderson, Nano-structure phosphorus-containing polyurethane dispersions: synthesis and crosslinking with melamine formaldehyde resin, *Polymer*, 44 (2003) 2631.
- [13] T. Solomons, *Organic Chemistry*, 6th ed., John Wiley & Sons, Inc., New York, 1996.
- [14] E. Sharmin, L. Imo, S. Ashraf and S. Ahmad, Acrylic-melamine modified DGEBA-epoxy coatings and their anticorrosive behavior, *Prog. Org. Coat.*, 50 (2004) 47.
- [15] D. Do, *Adsorption analysis: equilibria and kinetics*, Vol. 2, Imperial College Press, London, 1998.
- [16] S. Faust and O. Aly, *Adsorption processes for water treatment*, Butterworths, Boston, 1987.
- [17] M. Panayotova, Kinetics and thermodynamics of copper ions removal from wastewater by use of zeolite, *Waste Manage.*, 21 (2001) 671–676.
- [18] I. Tan, B. Hameed and A. Ahmad, Equilibrium and kinetic studies on basic dye adsorption by oil palm fibre activated carbon, *Chem. Eng. J.*, 127 (2007) 111–119.
- [19] S. Pramanik, S. Dey and P. Chattopadhyay, A new chelating resin containing azophenolcarboxylate functionality: synthesis, characterization and application to chromium speciation in wastewater, *Anal. Chim. Acta.*, 584 (2007) 469–476.
- [20] D. Prabhakaran and M. Subramanian, Enhanced metal extractive behavior using dual mechanism bifunctional polymer: an effective metal chelator, *Talanta*, 61 (2003) 431–437.
- [21] N. de Souza, J. Flores and J. Silva, Layer-by-layer films from tartrazine dye with bovine serum albumin, *Chem. Phys. Lett.*, 484 (2009) 33–36.
- [22] P. Hang and G. Brindley, Methylene blue absorption by clay minerals of surface areas and cation exchange capacities (clay-organic studies XVIII), *Clays Clay Miner.*, 18 (1970) 203–212.
- [23] A. Trochimczuk, B. Kolarz and D. Jermakowicz-Bartkowiak, Metal ion uptake by ion-exchange/chelating resins modified with cyclohexene oxide and cyclohexene sulphide, *Eur. Polym. J.*, 37 (2001) 559–564.
- [24] N. Ünlü and M. Ersoz, Removal of heavy metal ions by using dithiocarbamated-sporopollenin, *Sep. Purif. Technol.*, 52 (2007) 461–469.
- [25] J. Taylor, *An Introduction to Error analysis, The study of Uncertainties in Physical Measurements*, 2nd ed., University Science Books, Sausalito, CA, 1997.
- [26] Y. Ho, W. Chiu, C. Hsu and C. Huang, Sorption of lead ions from aqueous solution using tree fern as a sorbent, *Hydrometallurgy*, 73 (2004) 55–61.
- [27] A. Saeed, M. Iqbal and M. Akhtar, Removal and recovery of lead (II) from single and multimetal (Cd, Cu, Ni, Zn) solutions by crop milling waste (black gram musk), *J. Hazard. Mater.*, B 117 (2005) 65–73.
- [28] M. Martínez, N. Miralles, S. Hidalgo, N. Fiol, I. Villaescusa and J. Poch, Removal of lead(II) and cadmium(II) from aqueous solutions using grape stalk waste, *J. Hazard. Mater.*, B133 (2006) 203–211.
- [29] W. Adamsom, *Physical Chemistry of Surfaces*, 6th ed., Wiley, New York, 1997.
- [30] S.K. Parida and B.K. Mishra, Adsorption of Styryl Pyridinium Dyes on Silica Gel, *J. Colloid Interface Sci.*, 182(2) (1996) 473.

- [31] H. Boparai, M. Joseph and D. O'Carroll, Kinetics and thermodynamics of cadmium ion removal by adsorption onto nano zerovalent iron particles, *J. Hazard. Mater.*, 186 (2011) 458–465.
- [32] M. Wawrzekiewicz and Z. Hubicki, Removal of tartarazine from aqueous solutions by strongly basic polystyrene anion exchange resins, *J. Hazard. Mater.*, 164 (2009) 502–509.
- [33] J. Clayden, *Organic Chemistry*, Oxford University Press, Oxford, 2000.
- [34] J. Clayden, N. Greeves, S. Warren and P. Wothers, *Organic Chemistry*, Oxford University Press, Oxford, 2001.
- [35] M. Kara, H. Yuzer, E. Sabah and M.S. Celik, Adsorption of cobalt from aqueous solutions onto sepiolite, *Water Res.*, 37 (2003) 224–232.
- [36] S. Hasany and R. Ahmad, The potential of cost-effective coconut husk for the removal of toxic metal ions for environmental protection, *J. Environ. Manage.*, 81 (2006) 286–295.
- [37] F. Fu, Y. Xiong, B. Xie and R. Chen, Adsorption of Acid Red 73 on copper dithiocarbamate precipitate-type solid wastes, *Chemosphere*, 66 (2007) 1–7.
- [38] M. Özacar and İ. Şengil, A two stage batch adsorber design for methylene blue removal to minimize contact time, *J. Environ. Manage.*, 80 (2006) 372–379.
- [39] S. Yusan and S. Erenturk, Sorption behaviors of uranium (VI) ions on α -FeOOH, *Desalination*, 269 (2011) 58–66.
- [40] A. Chen, S. Liu, C. Chen and C. Chen, Comparative adsorption of Cu(II), Zn(II), and Pb(II) ions in aqueous solution on the crosslinked chitosan with epichlorohydrin, *J. Hazard. Mater.*, 154 (2008) 184–191.
- [41] W. Oliveira, A. Franca, L. Oliveira and S. Rocha, Untreated coffee husks as biosorbents for the removal of heavy metals from aqueous solutions, *J. Hazard. Mater.*, 152 (2008) 1073–1081.
- [42] B. Nandi, A. Goswami and M. Purkait, Adsorption characteristics of brilliant green dye on kaolin, *J. Hazard. Mater.*, 161 (2009) 387–395.
- [43] S. Gupta and K. Bhattacharyya, Adsorption of Ni(II) on clays, *J. Colloid. Interface Sci.*, 295 (2006) 21–32.
- [44] E. Malkoc, Ni(II) removal from aqueous solutions using cone biomass of *Thuja orientalis*, *J. Hazard. Mater.*, B137 (2006) 899–908.
- [45] C. Weng, C. Tsai, S. Chu and Y. Sharma, Adsorption characteristics of copper(II) onto spent activated clay, *Sep. Purif. Technol.*, 54 (2007) 187–197.
- [46] R. Liu, B. Zhang, D. Mei, H. Zhang and J. Liu, Adsorption of methyl violet from aqueous solution by halloysite nanotubes, *Desalination*, 268 (2011) 111–116.
- [47] B. Li, F. Su, H. Luo, L. Liang and B. Tan, Hypercrosslinked microporous polymer networks for effective removal of toxic metal ions from water, *Microporous. Mesoporous. Mater.*, 138 (2011) 207–214.
- [48] S. Azizian, Kinetic models of sorption: a theoretical analysis, *J. Colloid. Interface Sci.*, 276 (2004) 47–52.
- [49] M. Kamboh, I. Solangi, S. Sherazi and S. Memon, A highly efficient calix[4]arene based resin for the removal of azo dyes, *Desalination*, 268 (2011) 83–89.
- [50] F. Deniz and S. Saygideger, Removal of a hazardous azo dye (Basic Red 46) from aqueous solution by princess tree leaf, *Desalination*, 268 (2011) 6–11.
- [51] S. Nethaji and A. Sivasamy, Adsorptive removal of an acid dye by lignocellulosic waste biomass activated, carbon: equilibrium and kinetic studies, *Chemosphere*, 82 (2011) 1367–1372.
- [52] J. Rahchamani, H. Mousavi and M. Behzad, Adsorption of methyl violet from aqueous solution by polyacrylamide as an adsorbent: isotherm and kinetic studies, *Desalination*, 267 (2011) 256–260.
- [53] Y. Safa and H. Bhatti, Kinetic and thermodynamic modeling for the removal of Direct Red-31 and Direct, Orange-26 dyes from aqueous solutions by rice husk, *Desalination*, 272 (2011) 313–322.
- [54] L. Huang, Y. Sun, T. Yang and L. Li, Adsorption behavior of Ni (II) on lotus stalks derived active carbon by phosphoric acid activation, *Desalination*, 268 (2011) 12–19.
- [55] N. Mahmoodi, B. Hayati, M. Arami and C. Lan, Adsorption of textile dyes on Pine Cone from colored wastewater: kinetic, equilibrium and thermodynamic studies, *Desalination*, 268 (2011) 117–125.
- [56] Q. Zhong, Q. Yue, Q. Li, X. Xu and B. Gao, Preparation, characterization of modified wheat residue and its utilization for the anionic dye removal, *Desalination*, 267 (2011) 193–200.
- [57] D. Reddy, D. Ramana, K. Sessaiah and A. Reddy, Biosorption of Ni(II) from aqueous phase by *Moringa oleifera* bark, a low cost biosorbent, *Desalination*, 268 (2011) 150–157.
- [58] T. Sen and D. Gomez, Adsorption of zinc (Zn²⁺) from aqueous solution on natural bentonite, *Desalination*, 267 (2011) 286–294.
- [59] H. Boparai, M. Joseph and D. O'Carroll, Kinetics and thermodynamics of cadmium ion removal by adsorption onto nano zerovalent iron particles, *J. Hazard. Mater.*, 186 (2011) 458–465.
- [60] J. Fan, J. Zhang, C. Zhang, L. Ren and Q. Shi, Adsorption of 2,4,6-trichlorophenol from aqueous solution onto activated carbon derived from loessstrife, *Desalination*, 267 (2011) 139–146.